



Absorbing Boundary Condition and Soil-Tunnel Interaction for Numerical Modeling of Tunnel Response under Seismic Loading

Farzaneh Abedini¹ and Yazhou Xie^{2*}

¹ PhD Student, Department of Civil Engineering, McGill University, Montreal, Quebec, Canada

² Assistant Professor, Department of Civil Engineering, McGill University, Montreal, Quebec, Canada

* tim.xie@mcgill.ca (Corresponding Author)

ABSTRACT

Seismic risk assessment of tunnel infrastructure relies on high-fidelity numerical modeling of complete soil-tunnel systems and simulating their seismic responses under several ground motion excitations. In this respect, two crucial modeling tasks are to properly simulate the external boundary condition and the soil-tunnel interaction effect. First, the infinite soil medium, in reality, would attenuate seismic waves outward without reflecting them to the tunnel structure. A standard solution is to build a numerical model with a sufficiently large soil domain, which, however, will cause the model to be computationally demanding and intractable for large-scale seismic risk assessment. To deal with this, suitable absorbing boundary conditions (ABCs) need to be considered to dissipate a consistent amount of seismic energy. In addition, reliable seismic response prediction of the tunnel is also contingent on the level of resolution in capturing the soil-tunnel contact, gap opening, and friction behaviors at the interface. To this end, two-dimensional finite element models are built in ABAQUS to investigate to what degree different ABCs and soil-tunnel interface modeling strategies would change the seismic response of the tunnel. The case study is established against a cut-and-cover tunnel when subjected to earthquake loading in eastern Canada. Finally, tunnel responses under these different modeling considerations are compared to identify the most reliable simulation strategy. Results from the current study provide researchers and practitioners with a sound reference for assessing the seismic response of tunnel structures using numerical modeling.

Keywords: Absorbing Boundary Condition, Soil-Tunnel Interaction, Seismic Response Modeling, Tunnel, Finite Element Model

INTRODUCTION

Numerical simulation has been commonly applied to conduct seismic response analysis of complex geotechnical structures that engage substantial soil-structure interaction (SSI) under dynamic loading. On the other hand, developing numerical models can be challenging since they can only consider a finite number of nodes and elements [1]. Saint-Venant's principle suggests that the impact of an artificial boundary condition on local response should reduce with distance. However, when dealing with surrounding soils and rock under seismic loading, defining a sufficiently large domain to prevent wave reflection from returning to the region of interest is difficult due to the high speeds of these waves [2]. To this end, several methods have been developed, and one example is the use of absorbing boundary conditions (ABCs) to solve the problem through a finite modeling domain. In particular, ABCs efficiently absorb the energy of scattering seismic waves into the infinite medium [3-5].

ABCs can be classified into two categories, namely global and local boundaries. The choice between global and local boundary schemes depends on the desired level of accuracy, stability, and computational cost. The global scheme couples each boundary node to all other boundary nodes in space and time, whereas the local scheme considers that the solution at each time step only depends on the current node and its neighboring points. Methods for global boundaries include the boundary element method [6], the thin layer method [7], the exact Kirchhoff integration method [8], and the Dirichlet-to-Neumann method [9], etc. While these methods are generally more accurate, they require solving all boundary nodes simultaneously and are computationally expensive. In contrast, local boundaries are less precise, but they are much easier to implement, more computationally efficient, and, thereby, more attractive for engineering practices [2]. Examples of local artificial boundaries include viscous boundaries

[1, 10], viscous-spring boundaries [3, 11, 12], extrapolation boundaries, paraxial boundaries, multi-directional boundaries, and the perfectly matched layer (PML) [13, 14], etc. Furthermore, these local artificial boundaries can be classified into two types: the displacement type and the stress type. The transmitting boundary developed by Liao et al. [15] is the displacement-type boundary. In contrast, the viscous boundary [1], viscoelastic boundary [3], and high-order local time-domain boundary [16] belong to the stress type, which has gained widespread use and development due to their high accuracy and ease of implementation [17]. Over the years, various stress-type boundaries have been developed by incorporating dashpots. Lysmer and Kuhlemeyer [1] developed viscous dashpots to absorb incident waves [2]. Deeks and Randolph [11] proposed the first viscous-spring boundary to address SSI problems under dynamic action. Ye et al. [18] developed a new artificial boundary, namely a 2D arc-consistent viscous-spring artificial boundary (ACVAB) element, which improved the modeling accuracy.

Besides using dashpots, one method known as the infinite element method boundary (IEMB) has been developed to solve problems involving infinite domains. First proposed by Ungless [19] and later developed by Bettess [20], a mapping technique between global and local coordinates has been developed to create the Bettess element. Zienkiewicz et al. [21] further improved Bettess' work and proposed mapping infinite elements to solve problems that engage exterior waves. Yun et al. [22] later proposed a new method for solving pier-soil dynamic interaction in 2-D and 3-D domains using the IEMB approach in both frequency and time domains. This dynamic IEMB approach is found to have a better filtering effect on scattered waves than the viscous-spring artificial boundary (VSAB) method. The infinite element method can also be combined with the finite element method, with the former being used to simulate the far-field region and the latter being used to simulate the near-field region [23].

The PML is the other novel method that can absorb seismic energy. Initially introduced by Bérenger [24] for modeling electromagnetic wave fields, the PML consists of artificial material placed around the finite computational domain to fully absorb outgoing waves. This requires (1) no reflection at the interface of the interior and PML domain and (2) the transmitted outgoing waves inside the PML domain to be fully attenuated. Although the PML can theoretically absorb outgoing waves without any reflection, it is no longer completely reflectionless when the domain is discretized in the finite element model (FEM) in practice. Nonetheless, the PML method is still powerful for absorbing outgoing waves from various media, including elastic, poroelastic, anisotropic, and viscoelastic [25].

Different boundary treatments have been considered in the literature to deal with different dynamic loadings. However, it remains unknown which boundary condition is most suitable for seismic loads. This paper compares the applicability and efficiency of considering different boundary conditions to analyze soil-tunnel responses under seismic loading. In this regard, selecting the model dimension and a suitable boundary constitutes a trade-off between numerical accuracy and computational efficiency. This study starts with explaining different boundary implementations in the finite element software of ABAQUS. Subsequently, nonlinear time history analyses of soil-tunnel models using different modeling schemes at boundaries and soil-tunnel interfaces are conducted and compared to identify the optimal approach.

DIFFERENT ABSORBING BOUNDARY CONDITIONS

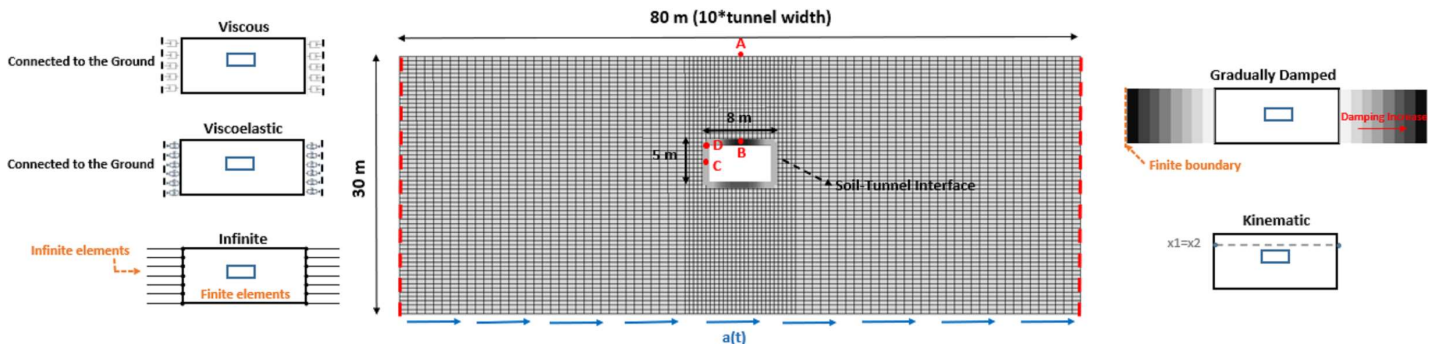


Figure 1. Numerical modeling of the tunnel with different boundaries and observation points

Viscous Boundary

As shown in Figure 1, a viscous boundary uses dashpots to absorb incident waves. Viscous boundaries replace the far field with viscous dampers. Notwithstanding its widespread acceptance, the viscous boundary has limitations. For instance, the viscous boundary produces permanent displacements at low frequencies since the entire model is statically unstable in space and can be shifted as a rigid body [26]. Several techniques have been developed to solve this problem, and one solution using the viscoelastic boundary [12] will be explained in the next section. To implement the viscous boundary in ABAQUS, dashpots

connected to the ground are defined in normal and tangential directions to the boundary nodes to absorb the impinging waves. The coefficients of dashpots for normal and tangential directions are defined as shown in Equation (1).

$$\begin{aligned} C_p &= \rho c_p A \\ C_s &= \rho c_s A \end{aligned} \quad (1)$$

where ρ stands for the medium density, A is the total area of each element around the considered node on the boundary, and c_p and c_s stand for longitudinal and shear wave velocities, respectively.

Viscoelastic Boundary

To solve the instability in low frequency [27] associated with the viscous boundary, a 2-D viscoelastic (spring-dashpot) boundary was developed by Deeks [28] and Liu [29], as shown in Figure 1. This boundary is developed based on cylindrical waves. Equation (2) shows the spring stiffness suggested by Liu et al. [3], and dashpot coefficients are similar to those given in Equation (1) [26]. In Equation (2), R is the perpendicular distance between the load and boundary, G is the shear modulus, and α_T and α_N are coefficients for springs along the tangential and normal directions, as listed in Table 1. This boundary combines springs and dashpots and is also known as VSAB and cone boundary. It enables energy absorption through the dashpot and deformation control through the spring connected to each node at the boundary. This boundary is most effective when the incident waves are perpendicular to the boundary. More details on the development of the boundary can be found in Liu et al.[3].

$$\begin{aligned} K_T &= \frac{\alpha_T G}{R} \\ K_N &= \frac{\alpha_N G}{R} \end{aligned} \quad (2)$$

Table 1. Recommended values for spring coefficients [3]

Modification Parameters	Value Range	Recommended Value
α_N	1.0 - 2.0	1.33
α_T	0.5-1.0	0.67

Infinite Element Boundary

As shown in Figure 1, infinite elements are another type of absorbing boundary for finite element models that provides *quiet* boundaries, as opposed to completely silent boundaries (i.e., perfect transmitters of all waveforms). Unlike dashpot/spring elements, infinite elements do not require the calculation of element coefficients [30]. They maintain the static boundary force generated at the beginning of the dynamic analysis, and far-field nodes will not move during the dynamic response stage. The ability of infinite elements to transmit energy out of the finite element mesh is optimized by making the finite-infinite element boundary orthogonal to the wave direction. While running dynamic analysis, the infinite elements have the static boundary stress as a constant without providing any stiffness. Consequently, there exists the rigid body motion of the modeled region. The infinite element boundary assumes that the response near the boundary has a small enough amplitude, resulting in linear solutions in the far field. As such, infinite elements should be positioned a reasonable distance away from the area of primary interest. ABAQUS provides first- and second-order infinite elements based on the work of Lysmer and Kuhlemeyer [1]. Boundary damping has been built into the infinite elements in ABAQUS, where details can be found in [31].

Gradually Damped Artificial Boundary

As the name implies, the gradually damped artificial boundary considers gradually increasing the damping to attenuate seismic waves. As shown in Figure 1, n -element sets are used to sequentially increase the damping coefficient/force from the innermost set to the one adjacent to the finite boundary. This avoids sudden damping increases that could cause the reflection of propagating waves. To determine the damping coefficient, an iterative procedure is employed to increase the damping until the responses obtained from two or more boundary cases show no significant difference. Sufficient damping is also needed to minimize the influence of the boundary [32].

Tied Degrees of Freedom Boundary Condition

Zienkiewicz et al. [33] introduced the tied degrees of freedom (TDOF) boundary condition, which constrains nodes at the same elevation on the two sides such that they move together (Figure 1). This boundary is also termed kinematic, tied, or periodic boundary in the literature. The TDOF boundary condition ensures that side nodes at the same elevation move together, making the common lateral displacement pattern in the soil possible. This boundary has been used in tunnel studies and validated against centrifuge tests [34, 35]. The method has been proven stable and compatible with advanced soil models.

NUMERICAL MODELLING

General Modeling Consideration

Seismic modeling of tunnel-soil systems presents unique challenges that require careful treatment of model boundaries and proper consideration to capture the dynamic interaction between tunnel and soil. This study adopts a typical example of a cut-and-cover tunnel to set up the numerical model and compare the tunnel's seismic performance against various absorbing boundary conditions applied at the lateral sides.

As shown in Figure 1, the tunnel is buried 10 m from the surface with a rectangular cross-section measuring 5 m in height and 8 m in width. The underground layers include clay, sand, and rock. The depth of the model is considered 30 m, assuming that the rigid engineering bedrock is reached. The model width is considered 80 m (i.e., 10 times the tunnel width), and 160 m, respectively, to minimize the size effect on boundary treatment. The model is considered in plane strain condition, and tunnel lining and soil are modeled using 2-D deformable beam and shell elements, respectively. The plane strain assumption considers negligible tunnel deformation in the longitudinal direction to save computational costs. The concrete for the tunnel lining has Young's modulus (E) of 22.8 GPa, a Poisson ratio (ν) of 0.2, and a density (ρ) of 2400 kg/m³. Reinforcing rebars are considered in the tunnel section with properties as shown in Table 2. A 30% reduction in the elastic modulus is also applied to capture the aging effect on the concrete tunnel.

Table 2. Rebar Properties

ρ (kg/m ³)	E (MPa)	ν	Yield Stress (MPa)
7850	210000	0.28	400

Choosing an appropriate constitutive model is crucial in capturing the behavior of the soil. Mohr-Coulomb has been most commonly used in modeling soils regarding seismic studies of tunnels [36-38]. An elastic-plastic soil behavior is considered herein by applying the Mohr-Coulomb constitutive model for the surrounding medium. It should be noted that more complex constitutive models did not always have superior performance, resulting from the difficulty of calibrating many more model parameters [39, 40]. Table 3 lists the considered soil profile and the associated soil properties, including Poisson ratio (ν), density (ρ), shear wave velocity (V_s), the module of elasticity (E), friction (ϕ) and dilation (ψ) angles, and cohesion (C). These material properties are selected based on a comprehensive literature review of typical geological conditions in East Canada.

Table 3. Soil and rock properties considered for the numerical model

Layer	Elevation (m)	V_s (m/s)	ρ (kg/m ³)	E (MPa)	ν	ϕ	ψ	C (Pa)
Sand	0-5	195	2000	200	0.3	35	5	1000
Clay 1	5-12	250	2000	325	0.3	25	0.1	30000
Clay 2	12-20	300	2000	470	0.3	25	0.1	50000
Rock	20-30	2650	2600	45000	0.2	35	5	10000

A 2% Rayleigh damping is also considered for the model at the first mode (f_1) and $5f_1$ based on the recommendations from [41-43]. Besides, the model needs to be meshed and discretized properly. This study considers a finer mesh for the region close to the tunnel. The size of the mesh is chosen such that the maximum element length equals one-eighth of the wavelength of the slowest body wave propagating in the elastic material, as shown in Equation (3) [10].

$$\lambda \leq \frac{V_s}{8f_{max}} \quad (3)$$

where V_s is shear wave velocity and f_{max} is the loading frequency; the predominant frequency of the earthquake loading varies depending on different factors, and earthquake ground motions in eastern Canada have relatively high frequency contents. This

calculated size for an element can ensure an efficient propagation of all the waveforms across the whole frequency range. The soil domain is meshed with 4-node quadrilateral (CPE4R) elements and the tunnel is meshed with beam elements (B21).

Modeling for Soil-Tunnel Interaction

The soil and tunnel would experience dynamic interaction at the interface [44, 45], which can significantly affect the seismic behavior of the tunnel [46]. Soil-tunnel interface can be modeled as the tied contact with no slip or the surface-to-surface contact that allows separation between two surfaces. The surface-to-surface contact simulates the tangential behavior using the penalty friction formulation, where the Coulomb friction coefficient is a function of the friction angle between soil and concrete. Normal behavior is modeled with hard contact. Modeling of the soil-tunnel interface depends on the type of soil. For instance, the separation of soil from the liner is meaningless for cohesionless soils; however, it is probable for cemented soils or undrained clays [47]. The assumption of rigid contact in the normal direction and frictional contact in the tangential direction for the contact model has been widely employed for numerical simulations of underground structures. Additional numerical models with one soil layer above the rock are considered to examine the impacts of soil-tunnel interaction. These models have different material properties assigned to the single soil layer, as shown in Table 4.

Table 4. Soil properties for interaction study

Soil Type	ρ (kg/m ³)	E (MPa)	ν	ϕ	ψ	C (Pa)
Sand A	2000	50	0.3	35	5	1000
Sand B	2000	200	0.3	35	5	1000
Clay A	2000	50	0.3	25	5	30000
Clay B	2000	300	0.3	25	5	30000

ANALYSIS RESULTS AND DISCUSSIONS

The study considers two sets of models, one with a width of 80 m and the other with 160 m. Each set of models is changed to have five different types of boundaries. The analyses for each model feature two steps. Namely, the gravity load is applied in a static general step followed by a dynamic implicit step in which the earthquake loading is applied through acceleration time history at the base. As such, the tunnel is modeled as being situated in a location with a gravity step to create an initial stress state around the tunnel. This two-step modeling approach has been widely used and verified through experiments [47-49]. In the dynamic analysis step, the input motion is selected from the synthetic motion database developed by Atkinson [50, 51], as shown in Figure 2.

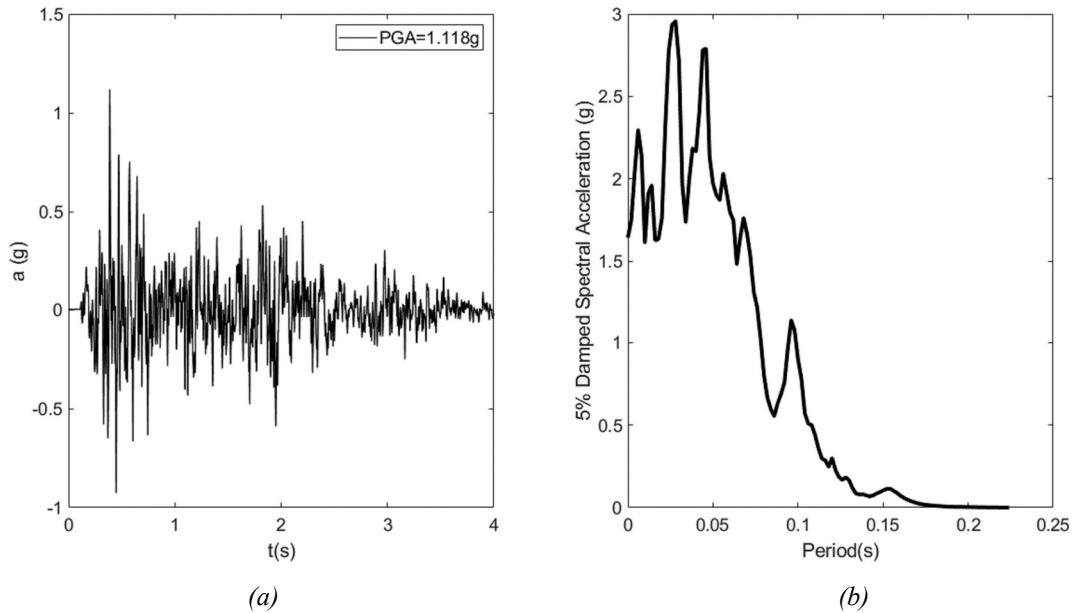


Figure 2. (a) Acceleration time history input, (b) 5% Damped spectra acceleration

Figure 3 to Figure 5 show acceleration responses at observation points A, B, and C provided in Figure 1. Some observations can be made from the results presented in these figures. First, the selection of the boundary condition affects the responses of the soil at point A (Figure 3), while it affects much less the responses of the tunnel at points B and C, as shown in Figure 4 and Figure 5. Second, the influence of the boundary layer is reduced when the width of the model is increased from 80 m to 160 m.

A large model helps reduce the boundary effect. Besides, all different boundary treatments yield consistent responses in the first two seconds where the maximum responses occur. Table 5 further compares the peak responses of points A, B, and C; the values in the parenthesis compute the relative percentage difference for each boundary against the kinematic boundary condition as a reference. As depicted in the tables, the relative differences range from 0.13% to 27.4% for the 80 m-width models and 0.27% to 7.74% for the 160 m-width model. The largest difference occurs at point A under the 80 m-width model with the infinite boundary condition.

Other than model accuracy, computational cost is of concern. The model with kinematic boundary is the most efficient one; it takes 20 minutes to complete the analysis for the 160 m-width model. In contrast, an infinite boundary takes approximately 2 hours to solve the same model. The computation time lies between 20 minutes and 2 hours for models developed with boundary conditions.

Also, small outward deformation was observed for the model with infinite boundaries owing to large strains. This makes its elastic response assumption questionable when dealing with large nonlinear responses under earthquake loading. Furthermore, defining an analysis involving consecutive static and dynamic analysis steps requires boundary transformation between these two steps, particularly for models with viscous and viscoelastic boundaries. Such a boundary transition may cause a sudden increase in acceleration and small deformations at the beginning of the dynamic analysis step on the boundary nodes, which needs to be taken into consideration. The gradually damped boundary requires multiple iterations to ensure that the motion is damped and the damping increase does not affect the results. As such, this boundary also needs to be implemented carefully. Therefore, it is preferable to adopt the kinematic boundary when (1) a computationally efficient model is needed for nonlinear time history analysis and (2) the maximum values are of interest for design and analysis.

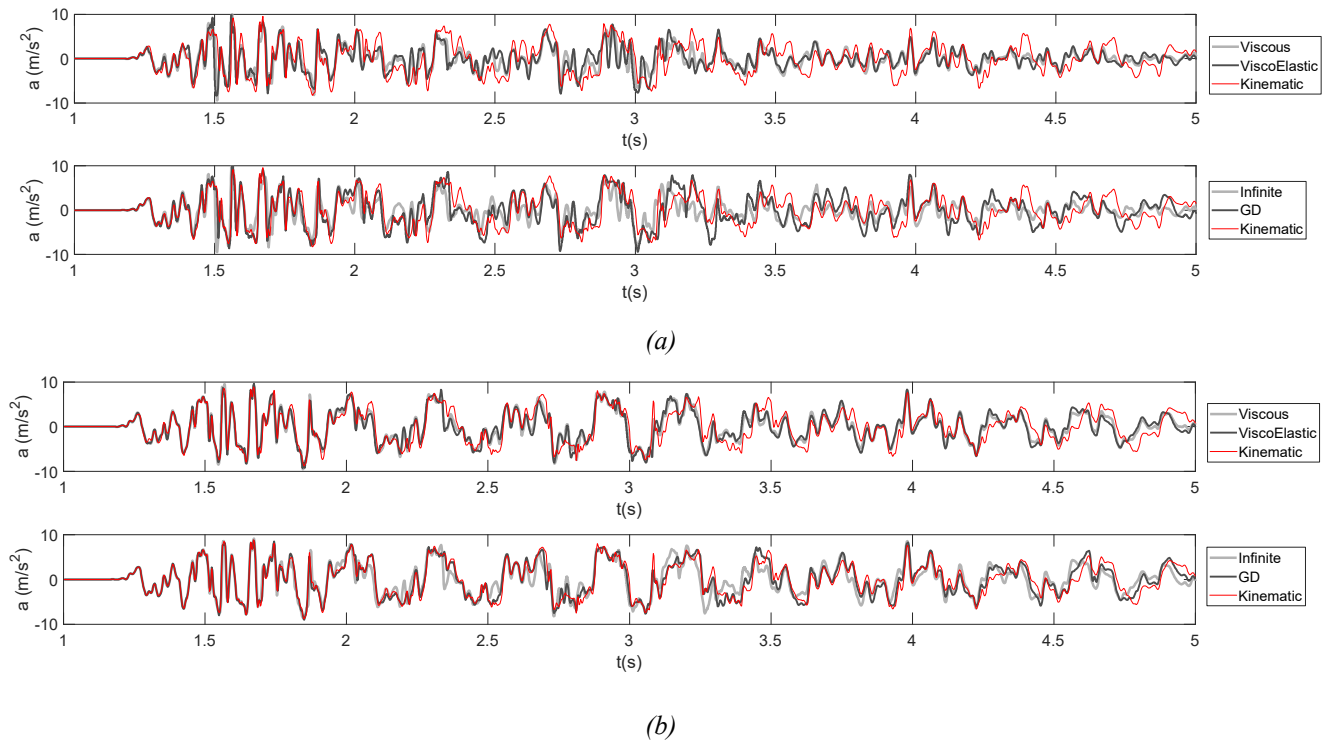


Figure 3. Acceleration response time history at point A in (a) 80-m and (b) 160-m models (GD refers to Gradually Damped)

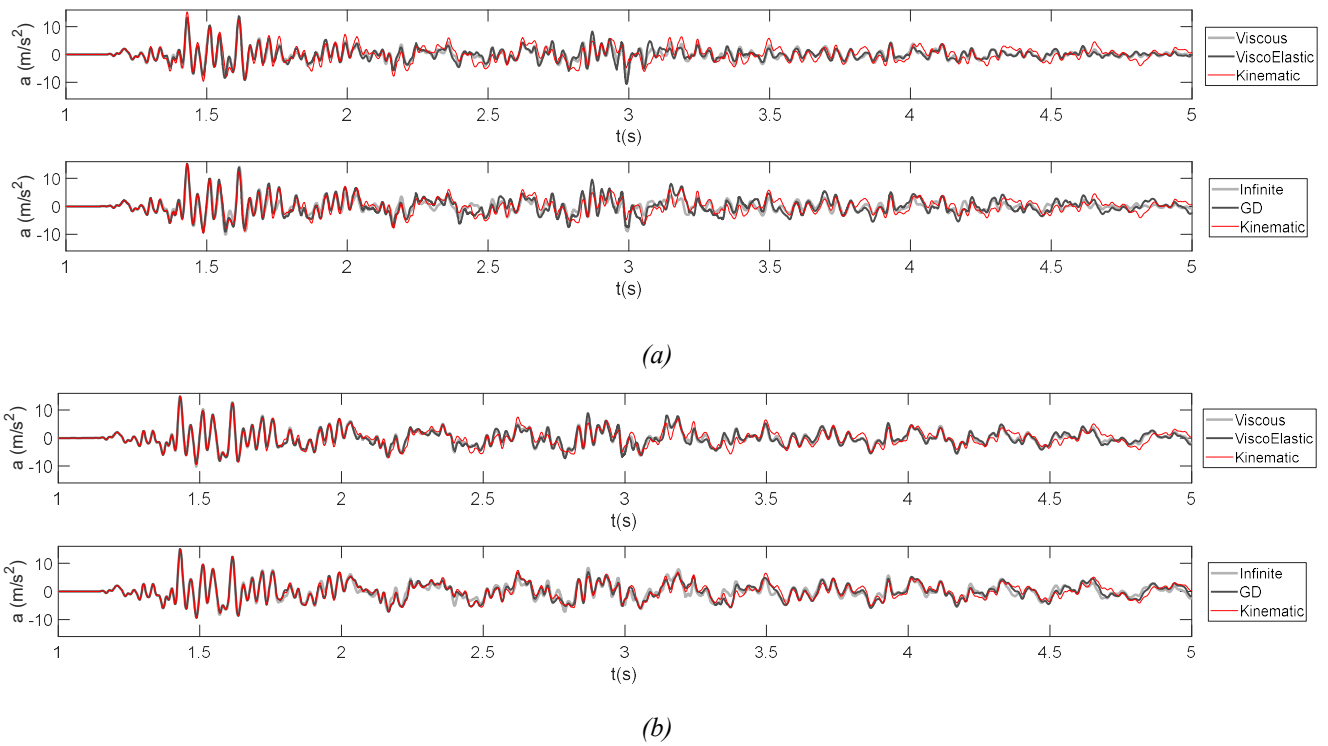


Figure 4. Acceleration response time history at point B in (a) 80-m and (b) 160-m models (GD refers to Gradually Damped)

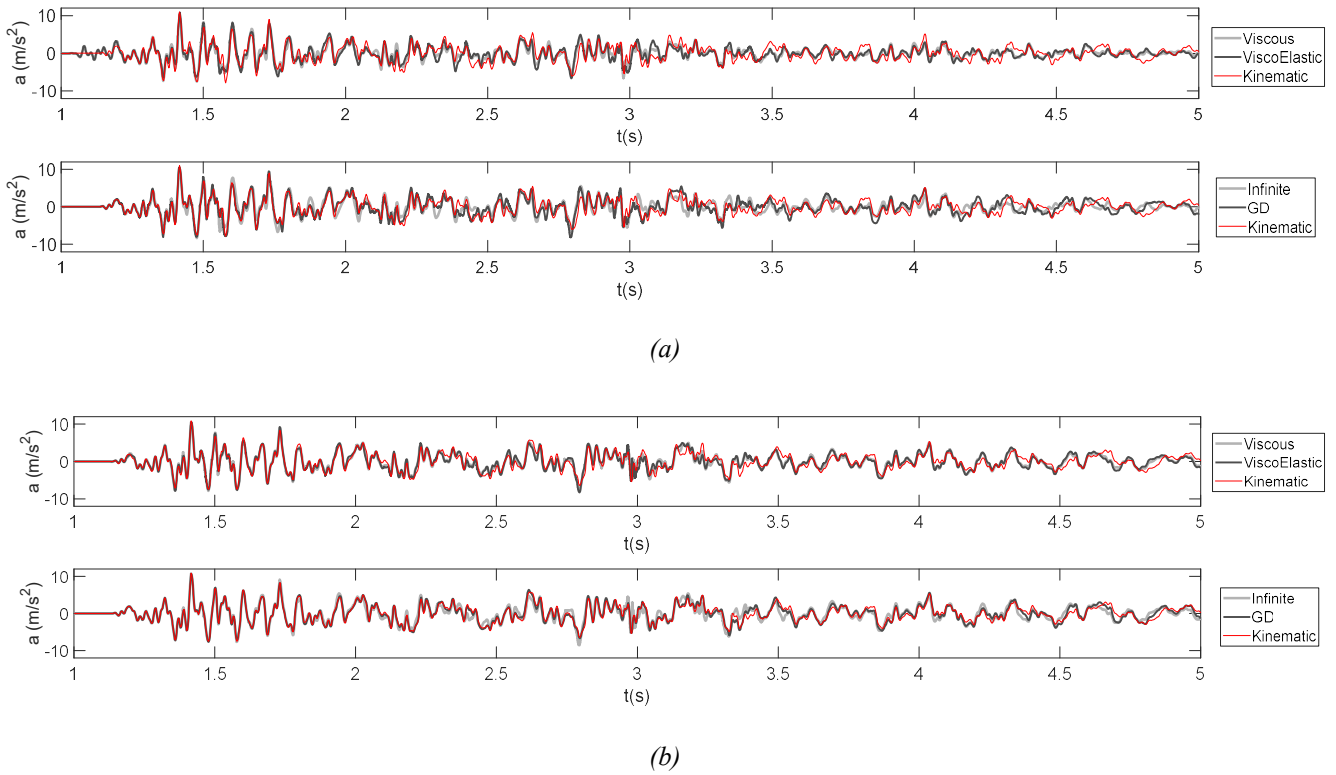


Figure 5. Acceleration response time history at point C in (a) 80-m and (b) 160-m models (GD refers to Gradually Damped)

Table 5. Maximum acceleration (m/s^2) at observation points A, B, and C under different boundaries

Point	Model Width	Viscous	Viscoelastic	Infinite	Gradually Damped	Kinematic
A	80 m	9.95 (+4.07%)	10.06 (+5.23%)	12.18 (+27.4%)	11.5 (+20.3%)	9.56
	160 m	9.57 (+7.4%)	9.60 (+7.74%)	9.19 (+3.14%)	9.02 (+1.23%)	8.91
B	80 m	12.45 (-18.83%)	13.76 (-10.3%)	14.17 (-7.62%)	15.32 (-0.13%)	15.34
	160 m	14.70 (-1.54%)	14.89 (-0.27%)	15.03 (+0.67%)	15.09 (+1.07%)	14.93
C	80 m	9.50 (-13.87%)	10.84 (-1.72%)	10.26 (-7%)	10.63 (-3.6%)	11.03
	160 m	10.53 (-3.038%)	10.53 (-3.03%)	10.78 (-0.73%)	10.67 (-1.75%)	10.86

Tied and surface-to-surface contact models are considered at the soil-tunnel interface to examine the soil-tunnel interaction effect. This study investigates the acceleration response at the wall roof corner of the tunnel (i.e., point D in Figure 1), which is expected to be mostly influenced by the modeling scheme at the interface. As illustrated in Figure 6, tying the soil and tunnel together results in lower accelerations. In contrast, the surface-to-surface contact model leads to higher accelerations when the soil and tunnel separate at the interface. The use of a lower friction angle/coefficient in the surface-to-surface contact model for the Clay-B case causes larger spikes and fluctuations in the tunnel response. The selection of an appropriate contact model, compatible with the soil behavior in reality (e.g., adhering and developing a gap or falling and filling the gap), is essential for reliably predicting the seismic responses of tunnels. For cases in which a more complex material model is assigned to the tunnel, soil-tunnel interaction can often result in peak response fluctuations.

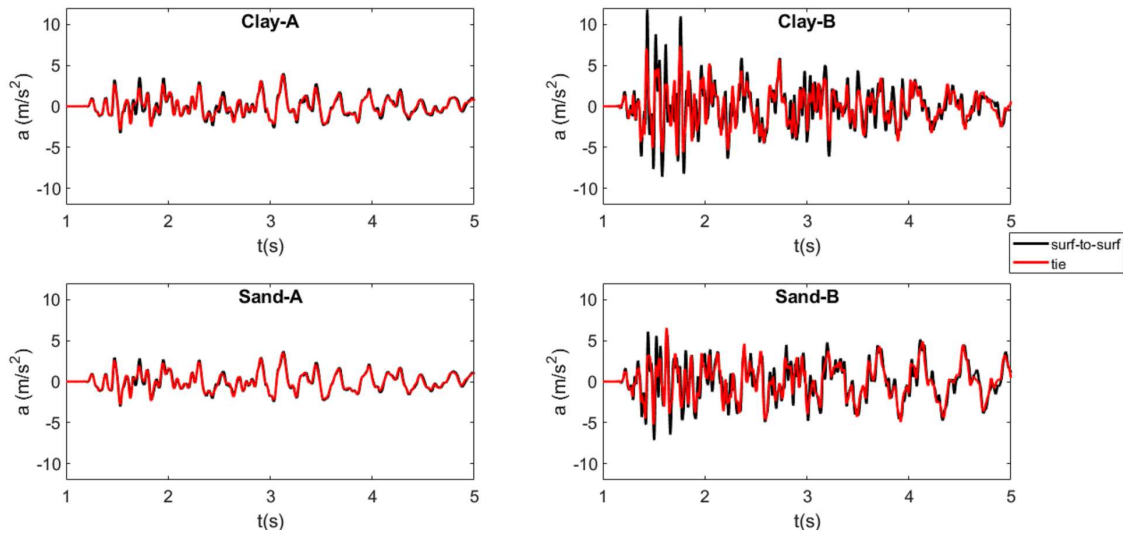


Figure 6. Acceleration for different interactions in different soil types at point D

CONCLUSIONS

Seismic simulation of tunnels requires proper modeling treatment at the lateral boundary and soil-tunnel interface. Appropriate absorbing boundary conditions (ABCs) are needed to dissipate a consistent amount of seismic energy and prevent seismic waves from being reflected back to the tunnel structure. This paper reviews different boundary modeling schemes and conducts nonlinear time history analyses based on soil-tunnel models developed in the finite element software of ABAQUS. Various ABCs for the seismic simulation of underground tunnels are investigated, considering accuracy, computational cost, and ease of implementation. The study identifies that the kinematic boundary is most suitable, as it demonstrates a reasonable level of accuracy, takes the lowest computation time, and is compatible with the advanced material model used for the tunnel. Furthermore, tying the soil and tunnel at the interface would result in smaller acceleration. Conversely, the surface-to-surface contact model would yield higher acceleration when soil and tunnel separate from each other under seismic shaking. Therefore, it remains essential to select an appropriate contact model that is physically consistent with the soil behavior in reality. This study offers researchers and practitioners a sound reference for selecting suitable boundary and interface models when analyzing and designing underground tunnels under earthquake loads.

ACKNOWLEDGMENTS

This research has been supported by the Mitacs Grant. Any opinions, findings, conclusions, or recommendations expressed in this paper are those of the authors and do not necessarily reflect the official views or policies of the funding agencies.

REFERENCES

- [1] Lysmer, J. and R.L. Kuhlemeyer, *Finite dynamic model for infinite media*. Journal of the engineering mechanics division, 1969. **95**(4): p. 859-877.
- [2] Nielsen, A.H. *Absorbing boundary conditions for seismic analysis in ABAQUS*. in *ABAQUS users' conference*. 2006.
- [3] Liu, J., et al., *3D viscous-spring artificial boundary in time domain*. Earthquake Engineering and Engineering Vibration, 2006. **5**(1): p. 93-102.
- [4] Wolf, J.P., *A comparison of time - domain transmitting boundaries*. Earthquake engineering & structural dynamics, 1986. **14**(4): p. 655-673.
- [5] Liao, Z., *Numerical simulation of near-field wave motion*. Advances in mechanics, 1997. **27**(2): p. 193-216.
- [6] Hall, W.S. and G. Oliveto, *Boundary element methods for soil-structure interaction*. 2003: Springer Science & Business Media.
- [7] Kausel, E., *Thin - layer method: Formulation in the time domain*. International journal for numerical methods in engineering, 1994. **37**(6): p. 927-941.
- [8] Givoli, D. and D. Cohen, *Nonreflecting boundary conditions based on Kirchhoff-type formulae*. Journal of Computational Physics, 1995. **117**(1): p. 102-113.
- [9] Givoli, D., *Exact representations on artificial interfaces and applications in mechanics*. 1999.
- [10] Kuhlemeyer, R.L. and J. Lysmer, *Finite element method accuracy for wave propagation problems*. Journal of the Soil Mechanics and Foundations Division, 1973. **99**(5): p. 421-427.
- [11] Deeks, A.J. and M.F. Randolph, *Axisymmetric time-domain transmitting boundaries*. Journal of Engineering Mechanics- Proceedings of the ASCE, 1994. **120**(1): p. 25-42.
- [12] Kellezi, L., *Local transmitting boundaries for transient elastic analysis*. Soil dynamics and earthquake engineering, 2000. **19**(7): p. 533-547.
- [13] Komatitsch, D. and R. Martin, *An unsplit convolutional perfectly matched layer improved at grazing incidence for the seismic wave equation*. Geophysics, 2007. **72**(5): p. SM155-SM167.
- [14] Zeng, Y., J. He, and Q. Liu, *The application of the perfectly matched layer in numerical modeling of wave propagation in poroelastic media*. Geophysics, 2001. **66**(4): p. 1258-1266.
- [15] Liao, Z.P. and H. Wong, *A transmitting boundary for the numerical simulation of elastic wave propagation*. International Journal of Soil Dynamics and Earthquake Engineering, 1984. **3**(4): p. 174-183.
- [16] Du, X. and M. Zhao, *A local time-domain transmitting boundary for simulating cylindrical elastic wave propagation in infinite media*. Soil Dynamics and Earthquake Engineering, 2010. **30**(10): p. 937-946.
- [17] Liu, J., et al., *Seismic wave input method for three-dimensional soil-structure dynamic interaction analysis based on the substructure of artificial boundaries*. Earthquake Engineering and Engineering Vibration, 2019. **18**: p. 747-758.
- [18] Ye, D., et al., *An Arc-Consistent Viscous-Spring Artificial Boundary for Numerical Analysis of Seismic Response of Underground Structures*. Shock and Vibration, 2022. **2022**: p. 1-12.
- [19] Ungless, R.F., *Infinite finite element*. 1973, University of British Columbia.
- [20] Bettess, P., *Infinite elements*. International Journal for numerical methods in engineering, 1977. **11**(1): p. 53-64.
- [21] Zienkiewicz, O., et al., *Mapped infinite elements for exterior wave problems*. International Journal for Numerical Methods in Engineering, 1985. **21**(7): p. 1229-1251.
- [22] Yun, C.-B., D.-K. Kim, and J.-M. Kim, *Analytical frequency-dependent infinite elements for soil-structure interaction analysis in two-dimensional medium*. Engineering structures, 2000. **22**(3): p. 258-271.
- [23] Xu, X., et al., *Study on earthquake damage mechanism of aqueduct structure based on different boundary*. Civil Engineering Journal, 2020(4).
- [24] Bérenger, J.-P., *Perfectly matched layer (PML) for computational electromagnetics*. Synthesis Lectures on Computational Electromagnetics, 2007. **2**(1): p. 1-117.
- [25] Poul, M.K. and A. Zerva, *Time-domain PML formulation for modeling viscoelastic waves with Rayleigh-type damping in an unbounded domain: Theory and application in ABAQUS*. Finite Elements in Analysis and Design, 2018. **152**: p. 1-16.
- [26] Ezzatyazdi, P. and H. Jahankhah, *Practical suggestions for 2D finite element modelling of soilstructure interaction problems*. in *Proc. 2nd European Conference on Earthquake Engineering and Seismology*. 2014.
- [27] Liu, J. and B. Li, *A unified viscous-spring artificial boundary for 3-D static and dynamic applications*. Science in China Series E Engineering & Materials Science, 2005. **48**: p. 570-584.
- [28] Deeks, A.J. and M.F. Randolph, *Axisymmetric time-domain transmitting boundaries*. Journal of Engineering Mechanics, 1994. **120**(1): p. 25-42.

- [29] Jingbo, L. and L. Yandong, *A direct method for analysis of dynamic soil-structure interaction based on interface idea*, in *Developments in geotechnical engineering*. 1998, Elsevier. p. 261-276.
- [30] Saleh Asheghabadi, M. and Z. Ali, *Infinite element boundary conditions for dynamic models under seismic loading*. Indian Journal of Physics, 2020. **94**: p. 907-917.
- [31] *ABAQUS Theory Manual* Available from: <https://classes.engineering.wustl.edu/2009/spring/mase5513/abaqus/docs/v6.6/books/stm/default.htm?startat=ch03s03at h68.html>.
- [32] Liu, G. and S.Q. Jerry, *A non-reflecting boundary for analyzing wave propagation using the finite element method*. Finite elements in analysis and design, 2003. **39**(5-6): p. 403-417.
- [33] Zienkiewicz, O., N. Bicanic, and F. Shen, *Earthquake input definition and the transmitting boundary conditions*. Advances in computational nonlinear mechanics, 1989: p. 109-138.
- [34] Argyroudis, S., et al. *Seismic fragility curves of shallow tunnels considering SSI and aging effects*. in *2nd Eastern European Tunnelling Conference "Tunnelling in a Challenging Environment*. 2014.
- [35] Tsinidis, G., et al., *Seismic response of box-type tunnels in soft soil: experimental and numerical investigation*. Tunnelling and Underground Space Technology, 2016. **59**: p. 199-214.
- [36] Cilingir, U. and S.G. Madabhushi, *A model study on the effects of input motion on the seismic behaviour of tunnels*. Soil Dynamics and Earthquake Engineering, 2011. **31**(3): p. 452-462.
- [37] Cilingir, U. and S.G. Madabhushi, *Effect of depth on the seismic response of square tunnels*. Soils and Foundations, 2011. **51**(3): p. 449-457.
- [38] Cilingir, U. and S.G. Madabhushi, *Effect of depth on seismic response of circular tunnels*. Canadian Geotechnical Journal, 2011. **48**(1): p. 117-127.
- [39] Bilotta, E., et al., *A numerical Round Robin on tunnels under seismic actions*. Acta geotechnica, 2014. **9**(4): p. 563-579.
- [40] Conti, R., G. Viggiani, and F. Perugini, *Numerical modelling of centrifuge dynamic tests of circular tunnels in dry sand*. Acta Geotechnica, 2014. **9**(4): p. 597-612.
- [41] Dolatshahi, K.M., A. Rezaie, and R. Rafiee-Dehkharghani, *Topology optimization of wave barriers for mitigation of vertical component of seismic ground motions*. Journal of Earthquake Engineering, 2020. **24**(1): p. 84-108.
- [42] Kwok, A.O., et al., *Use of exact solutions of wave propagation problems to guide implementation of nonlinear seismic ground response analysis procedures*. Journal of Geotechnical and Geoenvironmental Engineering, 2007. **133**(11): p. 1385-1398.
- [43] Hashash, Y.M. and D. Park, *Viscous damping formulation and high frequency motion propagation in non-linear site response analysis*. Soil Dynamics and Earthquake Engineering, 2002. **22**(7): p. 611-624.
- [44] Zaidan, Z.R., S.F. Al-Wakel, and Q.A. Hasan, *Numerical Analysis on Seismic Response of Multi-Stories Reinforced Concrete Buildings Under the Effect of Infinite Boundary of Soil-Structure Interaction*. Engineering and Technology Journal, 2019. **37**(12part (A) Engineering).
- [45] Tuladhar, R., *Seismic behavior of concrete pile foundation embedded in cohesive soil*. 2006, Ph. D. Dissertation, Saitama University, Japan.
- [46] Kouretzis, G.P., S.W. Sloan, and J.P. Carter, *Effect of interface friction on tunnel liner internal forces due to seismic S- and P-wave propagation*. Soil Dynamics and Earthquake Engineering, 2013. **46**: p. 41-51.
- [47] Tsinidis, G., *Response characteristics of rectangular tunnels in soft soil subjected to transversal ground shaking*. Tunnelling and Underground Space Technology, 2017. **62**: p. 1-22.
- [48] Huang, Z., et al., *Fragility assessment of tunnels in soft soils using artificial neural networks*. Underground Space, 2022. **7**(2): p. 242-253.
- [49] Tsinidis, G. and Ptilakis, K., *Toward the improvement of the RF method for the seismic analysis of rectangular tunnels*.
- [50] Atkinson, G.M., *Earthquake time histories compatible with the 2005 National building code of Canada uniform hazard spectrum*. Canadian Journal of Civil Engineering, 2009. **36**(6): p. 991-1000.
- [51] *Ground Motion Databases*. cited 2023; Available from: <https://www.seismotoolbox.ca/GMDatabases.html>.